J. Fluid Mech. (1978), *vol.* 87, *part* 2, *pp.* 209–231
Printed in Great Britain

The effects of eccentricity on torque and load in Taylor-vortex flow

By P. M. EAGLES,
Department of Mathematics, The City University, London

J. T. STUART
Mathematics Department, Imperial College, London

AND R. C. DIPRIMA
Department of Mathematical Sciences,
Rensselaer Polytechnic Institute, Troy, New York 12181

(Received 28 October 1977)

This paper extends two earlier papers in which DiPrima & Stuart calculated first (1972*b*) the critical Taylor number to order ϵ^2, where the eccentricity ϵ is proportional to the displacement of the axes of the circular cylinders, and second (1975) the torque and load to order ϵ associated with nonlinear effects of Taylor vortices. In the latter paper, it was shown that to order ϵ the torque arising from the Taylor vortices is identical with that for the concentric problem, which was first calculated, by a perturbation method, by Davey (1962). This deficiency is remedied in the present paper, where the calculation is taken to order ϵ^2. It is found that, as ϵ rises, the torque associated with the Taylor vortices falls slightly when we keep constant the percentage elevation of the Taylor number above the ϵ-dependent critical value. This result is in accordance with experimental observations by Vohr (1967, 1968). In addition, results of calculations of the pressure field developed by the Taylor-vortex flow in association with the eccentric geometry are presented; this is larger than in the concentric case owing to a Reynolds lubrication effect. Also given are the associated components of the load on the inner cylinder, but only for Taylor numbers close to the critical value.

One additional observation by Vohr, for cylinders with a mean ratio of the gap to the inner radius of 0·099, was that the maximum Taylor-vortex strength with $\epsilon = 0{\cdot}475$ occurred some 50° downstream of the maximum gap for a 20% elevation of the Taylor number above the critical value. Calculations in the two earlier papers (1972*b*, 1975) gave 90 and 76°, respectively, for that angle. Note that in the 1975 paper a geometrical correction of order ϵ was included. Here, with an additional modification of order ϵ due to the flow, this result is improved to 49° by the extended analysis presented, although the 'small' parameters are somewhat outside the range for which perturbation theory is expected to be valid.

1. Introduction

In three earlier papers (DiPrima & Stuart 1972*a*, *b*, 1975, hereafter designated I, II, III) two of the present authors developed theories for various aspects of the flow between two long rotating circular cylinders whose axes are displaced by an amount $(b-a)\epsilon$, where b and a are the radii of the outer and inner cylinders and ϵ $(0 \leqslant \epsilon < 1)$ is the eccentricity. This configuration is typical of the journal bearing and is of importance in lubrication technology. A summary of that earlier work is given by DiPrima & Stuart (1974).

In I the laminar flow was calculated as a series in two small parameters, namely the clearance ratio $\delta = (b-a)/a$ and a modified Reynolds number R_m proportional to $q_1(b-a)^2/a\nu$, where q_1 is the linear speed of the inner cylinder and ν is the kinematic viscosity. The work was really an extension, based on the Navier–Stokes equations, of Reynolds' classic work of 1886, and the eccentricity ϵ was allowed to take any value in the range $0 \leqslant \epsilon < 1$. However, for application to lubrication problems in liquids, the results are necessarily restricted to moderate values of ϵ, with δ small, since fluid cavitation occurs in the expanding region of the bearing for larger values of ϵ.

The linear stability of this steady flow was considered in II through a calculation to order ϵ^2 in which $\delta^{\frac{1}{2}}$ was held proportional to ϵ as the latter tended to zero. The resulting critical Taylor number, which depended on ϵ and δ, was acceptably close to many observations. Moreover, after a regrettable error in those calculations had been noted briefly at the end of III, the agreement with observation was found to be even closer; the corrected curves are presented in this paper in figures 2, 3 and 4. One additional prediction of II was that, since the stability problem is non-local, the position of maximum vortex activity lies not at the position of maximum gap, where the basic flow is most unstable, but is shifted substantially downstream. This result is qualitatively in accordance with observations by Vohr (1967, 1968).

Whereas the analysis in II was based on linearized perturbation equations, with the expansion taken to order ϵ^2, that in III used equations nonlinear in the Taylor-vortex velocity amplitude, but took the expansion only to order ϵ. The earlier technique of holding $\delta^{\frac{1}{2}}$ proportional to ϵ was again used, but with the additional constraint that the amplitude was made proportional to $\epsilon^{\frac{1}{2}}$. In this way nonlinear and eccentric effects were brought in *simultaneously* through a single amplitude equation. In the course of the analysis, it was found, not surprisingly in retrospect, that a stronger Taylor-vortex pressure field, compared with the concentric case, is developed by a 'lubrication' effect and that it is necessary to account for this pressure in order to satisfy boundary conditions on the velocity components at higher order. A related phenomenon occurs in the calculation of waves on water of finite depth (Benney & Roskes 1969; Davey & Stewartson 1974) and in the calculation of wave systems in plane Poiseuille flow (Davey, Hocking & Stewartson 1974), while Eagles (1971) noted the importance of a related pressure eigenfunction in the calculation of wavy vortices between concentric circular cylinders. In a similar sense, the discussion of pressure in plane Poiseuille flow by Stuart (1958, 1960) is relevant. Furthermore, a more abstract discussion is given by Kennett (1974).

The results of III were threefold: (i) after allowance for a geometrical effect of order ϵ, the position of maximum vortex activity (76°) was found to be closer to the

experimental situation (50°) than was the result in II (nearly 90°); (ii) the torque on the inner cylinder was precisely that of the concentric case when the calculation was taken to order ϵ; (iii) the load on the inner cylinder was calculated.

In the present paper, our object is to take the nonlinear calculation to order ϵ^2, and to calculate the changes brought about in (i), (ii) and (iii) above.

2. The basic equations and a perturbation expansion

In order to condense this paper and to avoid undue repetition, we shall refer to III for much of the detail and for many of the equations. Some geometrical and other details are, however, essential and will now be given. The two infinite cylinders with radii a and b, linear speeds q_1 and q_2 and with their centres a distance $ae = \epsilon(b-a)$ apart are shown in figure 1. Instead of polar co-ordinates (r, θ) centred on the inner cylinder, modified bipolar co-ordinates (ρ, ϕ) are used (Wood 1957), with the inner cylinder at $\rho = 1$ and the outer at $\rho = \beta = 1+\alpha$, while $\phi = 0$ and $\theta = 0$ are coincident at the maximum gap. The following parameters are relevant:

$$\left.\begin{aligned} \alpha(\delta,\epsilon) = \beta - 1 &= \delta(1-\epsilon^2)^{\frac{1}{2}}\{1-\tfrac{1}{2}\delta[1-(1-\epsilon^2)^{\frac{1}{2}}]\}+O(\delta^3), \\ \delta = (b-a)/a, &\qquad c = 2(q_1-q_2)/(q_1+q_2), \\ R_m = (q_1 a/\nu)\,\alpha^2, &\quad R_a = \tfrac{1}{2}(1+q_2/q_1)\,R_m, \\ T = (q_1 a/\nu)^2\,\alpha^3(1-q_2^2/q_1^2) &= 2cR_a^2/\alpha. \end{aligned}\right\} \tag{2.1}$$

The ρ and ϕ components u_ρ and u_ϕ of the basic laminar flow, whose nonlinear stability we are examining, are given in I and, in a form expanded in ϵ, in III(2.4)–(2.7). Thus

$$\left.\begin{aligned} u_\rho(x,\phi) &= \tfrac{1}{2}\alpha\epsilon(q_1+q_2)\,U(x,\phi), \quad u_\phi(x,\phi) = \tfrac{1}{2}(q_1+q_2)\,V(x,\phi), \\ U(x,\phi) &= 2(x^2-\tfrac{1}{4})\,(x-\tfrac{1}{4}c)\sin\phi + O(\epsilon), \\ V(x,\phi) &= V_0(x)+\epsilon V_1(x,\phi)+\epsilon^2[V_{20}(x)+kT^{\frac{1}{2}}V_{21}(x,\phi)+k^2c^2V_{22}(x)]+O(\epsilon^3), \end{aligned}\right\} \tag{2.2}$$

$$\rho - 1 = \alpha(x+\tfrac{1}{2}), \tag{2.3}$$

where the functions V_0, V_1, V_{20}, V_{21} and V_{22} are given by III(2.7). The parameter k is defined by

$$\alpha^{\frac{1}{2}} = k\epsilon(2c)^{\frac{1}{2}}, \tag{2.4}$$

while the factor $T^{\frac{1}{2}}$ arises from $R_a = (\alpha T/2c)^{\frac{1}{2}}$ with k held fixed as $\alpha, \epsilon \to 0$ subject to (2.4).

Perturbations from the above velocity field, together with the axial velocity component u_ξ and the kinematic pressure p', are given by the following formulae, where $a\alpha\xi$ is the axial co-ordinate, $\tau a^2\alpha^2/\nu$ is the time and $P(x,\phi)$ is proportional to the pressure field of the basic flow:

$$\left.\begin{aligned} u_\rho(x,\phi,\xi,\tau) &= \tfrac{1}{2}\alpha\epsilon(q_1+q_2)\,U(x,\phi)+(\nu/a\alpha)\,u(x,\phi,\xi,\tau), \\ u_\phi(x,\phi,\xi,\tau) &= \tfrac{1}{2}(q_1+q_2)\,V(x,\phi)+(q_1-q_2)\,v(x,\phi,\xi,\tau), \\ u_\xi(x,\phi,\xi,\tau) &= (\nu/a\alpha)\,w(x,\phi,\xi,\tau), \\ p'(x,\phi,\xi,\tau) &= (\nu q_1/a\alpha^2)\,P(x,\phi)+(\nu^2/a^2\alpha^2)\,p(x,\phi,\xi,\tau). \end{aligned}\right\} \tag{2.5}$$

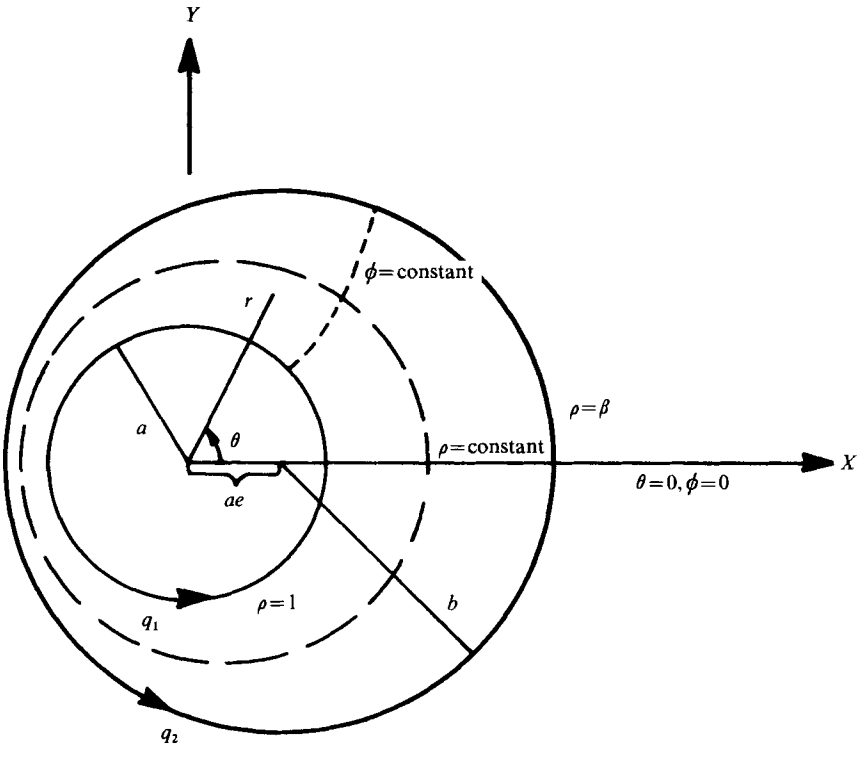

FIGURE 1. Geometry and co-ordinate systems.

The above scalings are suggested by the work of Stuart (1958) and Davey (1962) on the concentric nonlinear problem.

The governing nonlinear partial differential equations for u, v, w and p are given in III(2.13)–(2.18), while the required Jacobian J of the conformal transformation is defined in II(2.6). In III it is suggested and confirmed that an expansion of the following form is appropriate for the steady solution, where $\epsilon \to 0$ with k held fixed subject to (2.4):

$$\{u, v, w\} = \epsilon^{\frac{1}{2}} \sum_{n=0}^{\infty} \epsilon^{\frac{1}{2}n} \{u_n(x, \phi, \xi), v_n(x, \phi, \xi), w_n(x, \phi, \xi)\}, \tag{2.6}$$

$$p = \frac{T^{\frac{1}{2}} \epsilon^{-2}}{4ck^3} \left[\int_0^{\phi} q_0(\phi)\, d\phi + \epsilon \int_0^{\phi} q_1(\phi)\, d\phi + O(\epsilon^2) \right] + \epsilon^{\frac{1}{2}} \sum_{n=0}^{\infty} \epsilon^{\frac{1}{2}n} p_n(x, \phi, \xi) + \text{constant}, \tag{2.7}$$

$$T = \sum_{n=0}^{\infty} \epsilon^n T_n, \quad R_a = k\epsilon [T_0^{\frac{1}{2}} + \epsilon T_1 / 2T_0^{\frac{1}{2}} + O(\epsilon^2)]. \tag{2.8}$$

We remind the reader that the term in p multiplied by $\epsilon^{\frac{1}{2}}$ is the 'usual' Taylor-vortex pressure field, while the term in p multiplied by ϵ^{-2} is a 'lubrication' or Reynolds pressure field. As explained in III (§ 3), the latter arises from conservation of mass flux or equivalently from the satisfaction of boundary conditions on the velocity. Other relevant work has been cited already in § 1.

Substitution of (2.6)–(2.8) into the governing differential equations yields sets of equations at orders $\epsilon^{\frac{1}{2}n}$; these are given for $n = 1$, 2 and 3 in III(3.17)–(3.26). The first Reynolds pressure function $q_0(\phi)$ appears at order ϵ and drives a plane Poiseuille component of velocity at that order. However, $q_0(\phi)$ is determined only when the

continuity equation at order ϵ^2 (III, 3.15) is used to satisfy the velocity boundary condition at that order.

In the present paper, we take the Taylor number, velocity and 'usual' Taylor-vortex pressure expansions (2.6)–(2.8) to $n = 4$, but we need to consider the continuity condition for $n = 5$ in order to determine the Reynolds pressure function $q_1(\phi)$. We shall not give all the equations in detail, but the general principles and the solutions are described in § 3.

3. Solutions and associated computations

It can be seen from III(4.1) that the functions u_0, v_0, w_0 and p_0 [the 0-functions of (2.6) and (2.7)] describing the Taylor vortex are periodic in ξ with wavenumber λ, from III(4.2) that the 1-functions are the sum of parts independent of ξ and periodic in ξ with wavenumber 2λ, and from III(4.16) that the 2-functions are the sum of periodic parts with wavenumbers λ and 3λ. For the coefficients of these Fourier terms, which are functions of x and ϕ, the differential equations involve x derivatives only, with ϕ as a parameter at each stage. At lowest order the solution of a homogeneous eigenvalue problem is determined only up to a multiplicative function of ϕ, which is determined at a higher order in the expansion by means of an integrability condition. The ϕ dependence of the succeeding inhomogeneous equation is determined by the ϕ dependence of the forcing term, special attention being paid to the cases in which the linear operator repeats that of the original eigenvalue problem (parts of the solution which are periodic in ξ with wavenumber λ), and to the mean flow equations, where account must be taken of the 'lubrication' pressure.

The expansion procedure is explained in § 4 of III. The form of the expansion required to go to higher order in ϵ is as follows, where $C_{n\lambda} = \cos n\lambda\xi$ and $S_{n\lambda} = \sin n\lambda\xi$:

$$u_0 = -B(\phi)f_0(x)C_{1\lambda}, \quad v_0 = B(\phi)g_0(x)C_{1\lambda}, \quad w_0 = B(\phi)h_0(x)S_{1\lambda}, \quad p_0 = B(\phi)l_0C_{1\lambda}; \tag{3.1}$$

$$u_1 = -B^2(\phi)f_{12}(x)C_{2\lambda}, \tag{3.2a}$$

$$v_1 = B^2(\phi)g_{10}(x) + 3Q_0\Gamma_3\Gamma_4^{-1}T_1(x^2-\tfrac{1}{4}) + B^2(\phi)g_{12}(x)C_{2\lambda}, \tag{3.2b}$$

$$w_1 = B^2(\phi)h_{12}(x)S_{2\lambda}, \tag{3.2c}$$

$$p_1 = B^2(\phi)l_{10}(x) + 6Q_0\Gamma_3\Gamma_4^{-1}T_1l_{100}(x) + B^2(\phi)l_{12}(x)C_{2\lambda} + \text{constant}; \tag{3.2d}$$

$$\begin{aligned} u_2 = &-[B_1(\phi)f_0(x) + T_1B(\phi)f_{211}(x) + B(\phi)\cos\phi f_{212}(x) + B^3(\phi)f_{213}(x)]C_{1\lambda} \\ &- B^3(\phi)f_{23}(x)C_{3\lambda}, \end{aligned} \tag{3.3}$$

$$\begin{aligned} v_2 = &[B_1(\phi)g_0(x) + T_1B(\phi)g_{211}(x) + B(\phi)\cos\phi g_{212}(x) \\ &+ B^3(\phi)g_{213}(x)]C_{1\lambda} + B^3(\phi)g_{23}(x)C_{3\lambda}, \end{aligned} \tag{3.3b}$$

$$\begin{aligned} w_2 = &[B_1(\phi)h_0(x) + T_1B(\phi)h_{211}(x) + B(\phi)\cos\phi h_{212}(x) \\ &+ B^3(\phi)h_{213}(x)]S_{1\lambda} + B^3(\phi)h_{23}(x)S_{3\lambda}, \end{aligned} \tag{3.3c}$$

$$p_2 = [B_1(\phi)l_0(x) + T_1B(\phi)l_{211}(x) + B(\phi)\cos\phi l_{212}(x) + B^3(\phi)l_{213}(x)]C_{1\lambda} + B^3(\phi)l_{23}(x)C_{3\lambda}; \tag{3.3d}$$

$$\begin{aligned} u_3 = &-[B^4(\phi)f_{301}(x) + B^2(\phi)\cos\phi f_{302}(x) + T_1B^2(\phi)f_{304}(x)] - [B^4(\phi)f_{321}(x) \\ &+ B^2(\phi)\cos\phi f_{322}(x) + 2B_1(\phi)B(\phi)f_{12}(x) + T_1B^2(\phi)f_{324}(x)]C_{2\lambda} - B^4(\phi)f_{341}(x)C_{4\lambda}, \end{aligned} \tag{3.4a}$$

$$v_3 = B^4(\phi)\, g_{301}(x) + B^2(\phi)\cos\phi\, g_{302}(x) + 2B_1(\phi)\, B(\phi)\, g_{10}(x)$$
$$+ T_1 B^2(\phi)\, g_{304}(x) + \tfrac{1}{2}[\sigma_1 - 6Q_0\Gamma_3\Gamma_4^{-1}T_1\cos\phi]\,(x^2 - \tfrac{1}{4})$$
$$+ [B^4(\phi)\, g_{321}(x) + B^2(\phi)\cos\phi\, g_{322}(x) + 2B_1(\phi)\, B(\phi)\, g_{12}(x)$$
$$+ T_1 B^2(\phi)\, g_{324}(x)]\, C_{2\lambda} + B^4(\phi)\, g_{341}(x)\, C_{4\lambda}, \tag{3.4b}$$

$$w_3 = [B^4(\phi)\, h_{321}(x) + B^2(\phi)\cos\phi h_{322}(x) + 2B_1(\phi)\, B(\phi)\, h_{12}(x)$$
$$+ T_1 B^2(\phi)\, h_{324}(x)]\, S_{2\lambda} + B^4(\phi)\, h_{341}(x)\, S_{4\lambda}, \tag{3.4c}$$

$$p_3 = B^4(\phi)\, l_{301}(x) + B^2(\phi)\cos\phi l_{302}(x) + 2B_1(\phi)\, B(\phi)\, l_{10}(x)$$
$$+ T_1 B^2(\phi)\, l_{304}(x) + 18T_0Q_0\Gamma_3\Gamma_4^{-1}T_1\cos\phi \int_{-\frac{1}{2}}^{x} (x^2 - \tfrac{1}{4})^2\, dx$$
$$+ T_1^2 l_{306}(x) + \sigma_1 l_{100}(x) + [B^4(\phi)\, l_{321}(x) + B^2(\phi)\cos\phi l_{322}(x) + 2B_1(\phi)\, B(\phi)\, l_{12}(x)$$
$$+ T_1 B^2(\phi)\, l_{324}(x)]\, C_{2\lambda} + B^4(\phi)\, l_{341}(x)\, C_{4\lambda}. \tag{3.4d}$$

The sets of functions (f_0, g_0, h_0, l_0), $(f_{12}, g_{12}, h_{12}, l_{12}), \ldots$ are calculated sequentially. For a given value of λ, the parameter T_0 of (2.8) is determined as the solution of a linear eigenvalue problem with associated eigenfunction (f_0, g_0, h_0, l_0) as given in III(4.1). The parameters Q_0, Γ_3 and Γ_4 are defined in III, while σ_1 is determined by (3.16). The functions $B(\phi)$ and $B_1(\phi)$ are given by the solution of first-order differential equations arising from integrability conditions, as mentioned earlier in this section. They will be discussed later, together with the choice of the constants T_1 and T_2.

In carrying out the calculations, we found it convenient to follow the method of Eagles (1971) and rewrite the disturbance equations as a system of six first-order partial differential equations for u, v, w, p, $\partial v/\partial x$ and $\partial w/\partial x$. This makes the formal analytical calculations simpler, and is consistent with standard methods for solving the resulting ordinary differential equations. It is clear from (3.1)–(3.4) that the x-dependent functions appearing in the ordinary differential equations have the following associations, where suffixes have been omitted: $f \sim u$, $g \sim v$, $h \sim w$ and $l \sim p$, the additional variables being $r \sim \partial v/\partial x$ and $s \sim \partial w/\partial x$.

The generic structure for each set of ordinary differential equations is

$$D\mathbf{U} - \mathbf{A}^{(n)}\mathbf{U} = \mathbf{W}, \tag{3.5}$$

where D denotes d/dx, $\mathbf{U}^{\mathrm{T}} = (l, r, s, f, g, h)$, $r = Dg$, $s = Dh$, $\mathbf{W}^{\mathrm{T}} = (L, R, S, F, G, H)$ and $\mathbf{A}^{(n)}$ is a matrix given by

$$\mathbf{A}^{(n)} = \begin{pmatrix} 0 & 0 & -n\lambda & n^2\lambda^2 & T_0V_0(x) & 0 \\ 0 & 0 & 0 & 1 & n^2\lambda^2 & 0 \\ -n\lambda & 0 & 0 & 0 & 0 & n^2\lambda^2 \\ 0 & 0 & 0 & 0 & 0 & n\lambda \\ 0 & 1 & 0 & 0 & 0 & 0 \\ 0 & 0 & 1 & 0 & 0 & 0 \end{pmatrix}. \tag{3.6}$$

The column vector $\mathbf{W}$ represents the inhomogeneity arising from the nonlinear interaction. The boundary conditions are

$$(\beta_1): \quad (n \neq 0) \quad f = g = h = 0 \quad \text{at} \quad x = \pm\tfrac{1}{2}, \tag{3.7}$$

$$\left.\begin{aligned} (\beta_0): \quad (n = 0) \quad g = h &= 0 \quad \text{at} \quad x = \pm\tfrac{1}{2}, \\ f = l &= 0 \quad \text{at} \quad x = -\tfrac{1}{2}. \end{aligned}\right\} \tag{3.8}$$

In the generic problem (3.5) the functions $\mathbf{U}$ and $\mathbf{W}$ have an associated suffix of one, two or three digits depending on the order in the expansion in ϵ, the harmonic in ξ and the power of the amplitude function $B(\phi)$.

In addition, it is necessary to consider the adjoint problem for $n = 1$, namely

$$D\mathbf{U}_a + \mathbf{A}^{(1)\mathrm{T}}\mathbf{U}_a = 0, \tag{3.9}$$

subject to the boundary conditions

$$(\beta_a): \quad l_a = r_a = s_a = 0 \quad \text{at} \quad x = \pm\tfrac{1}{2}. \tag{3.10}$$

In a comparison with II(5.7)–(5.9), it should be noted that $l_a = \lambda^2 f_0^+$, $r_a = g_0^+$ and $s_a = \lambda D f_0^+$.

Rather than give complete details, we treat two specimen problems $S1$ and $S2$.

$$\left.\begin{aligned}
(S1): \quad & D\mathbf{U}_{10} - \mathbf{A}^{(0)}\mathbf{U}_{10} = \mathbf{W}_{10} \quad \text{with} \quad (\beta_0), \\
& L_{10} = -\lambda f_0 h_0 + \tfrac{1}{4} c T_0 g_0^2, \\
& R_{10} = -6Q_0 - \tfrac{1}{2}(f_0 r_0 + \lambda g_0 h_0), \\
& S_{10} = F_{10} = G_{10} = H_{10} = 0, \\
& Q_0 = \int_{-\frac{1}{2}}^{\frac{1}{2}} dx \int_{-\frac{1}{2}}^{x} f_0 g_0 \, dx - \frac{1}{2}\int_{-\frac{1}{2}}^{\frac{1}{2}} f_0 g_0 \, dx,
\end{aligned}\right\} \tag{3.11}$$

with a check constraint

$$\int_{-\frac{1}{2}}^{\frac{1}{2}} g_{10}(x)\, dx = 0.$$

This is a re-formulation of III(4.6)–(4.15), with f_0 and g_0 defined by III(4.1) while $h_0 = \lambda^{-1} D f_0$ and $r_0 = D g_0$. The normalizations imposed here on that eigenvalue problem and its adjoint II(5.7)–(5.9) are $g_0 = 1$ at $x = 0$ and $g_a = 1$ at $x = -\frac{1}{2}$. Note the contrast with the normalizations of II (p. 407). The present nonlinear results, however, can be compared directly with III(4.30), since the fundamental (f_0, g_0) normalizations are the same.

$$\left.\begin{aligned}
(S2): \quad & D\mathbf{U}_{211} - \mathbf{A}^{(1)}\mathbf{U}_{211} = \mathbf{W}_{211} \quad \text{with} \quad (\beta_1), \\
& L_{211} = V_0 g_0 + 3cQ_0 T_0 \Gamma_3 \Gamma^{-1}(x^2 - \tfrac{1}{4}) g_0 + \Gamma_3 \Gamma_4' \Gamma_4^{-1}(V_0 f_0 - c r_0), \\
& R_{211} = -6Q_0 \Gamma_3 \Gamma_4^{-1} x f_0 + \Gamma_3 \Gamma_4' \Gamma_4^{-1} V_0 g_0, \\
& S_{211} = \Gamma_3 \Gamma_4' \Gamma_4^{-1} V_0 h_0, \quad F_{211} = \Gamma_3 \Gamma_4' \Gamma_4^{-1} c g_0, \quad G_{211} = H_{211} = 0.
\end{aligned}\right\} \tag{3.12}$$

In addition, Q_0 is defined by (3.11) and Γ_3, Γ_4 and Γ_4' by III(4.23) and (4.27).

There is a check constraint on each of $g_{301}(S)$, $g_{302}(S)$ and $g_{304}(x)$, namely that

$$\int_{-\frac{1}{2}}^{\frac{1}{2}} g_{30i}(x)\, dx = 0, \quad i = 1, 2, 4. \tag{3.13}$$

These constraints and the corresponding one in (3.11) for g_{10} ensure that mass flux is conserved and that the boundary conditions on the component of flow independent of ξ are satisfied.

The amplitude function $B(\phi)$ is given by III(4.22)–(4.26), while $B_1(\phi)$ must satisfy

$$\begin{aligned}
& kT_0^{\frac{1}{2}} d[B_1(\phi)/B(\phi)]/d\phi + 2\Gamma_4' B^2(\phi)\,[B_1(\phi)/B(\phi)] \\
& \qquad = -\Gamma_{417}\cos 2\phi - \Gamma_{4110} T_1 \cos\phi - \Gamma_{4111} T_1^2 + \Gamma_5 \sigma_1 - \Gamma_{4115} B^4(\phi).
\end{aligned} \tag{3.14}$$

Here σ_1 is chosen to ensure that the pressure-gradient function, namely

$$q_1(\phi) = I_{301}B^4(\phi) + I_{302}B^2(\phi)\cos\phi - 12Q_0B_1(\phi)B(\phi) + I_{304}T_1B^2(\phi) - 12Q_0\Gamma_3\Gamma_4^{-1}T_1\cos\phi + \sigma_1, \tag{3.15}$$

where the I_{30i}, $i = 1, 2, 4$, are certain integrals involving the **U** functions, satisfies

$$\int_0^{2\pi} q_1(\phi)\,d\phi = 0, \tag{3.16}$$

so that the pressure is single valued. The corresponding $q_0(\phi)$ function is given by III(4.7) and (4.27).

The coefficients Γ_{417}, Γ_{4110}, Γ_{4111} and Γ_{4115} arise as quotients of integrals when the integrability conditions for the appropriate differential systems are applied. They are of the form

$$\Gamma_{41i} = -\Gamma_0^{-1}\int_{-\frac{1}{2}}^{\frac{1}{2}} (l_aL_{41i} + r_aR_{41i} + s_aS_{41i} + f_aF_{41i})\,dx, \quad i = 7, 10, 11, 15, \tag{3.17}$$

$$\Gamma_0 = -\int_{-\frac{1}{2}}^{\frac{1}{2}} [l_a(V_0f_0 - cr_0) + r_aV_0g_0 + s_aV_0h_0 + f_acg_0]\,dx, \tag{3.18}$$

in which the L, R, S and F functions depend on the functions in (3.1)–(3.4). The parameter Γ_5 is given in III(4.23). The coefficient T_2 in the expansion (2.8) has been chosen to be identical with that of linearized theory given in II(5.41), after correction of II(5.31) according to p. 110 of III, so that ϵT_1 represents the elevation of the Taylor number above its critical value of $T_0 + \epsilon^2T_2$ to order ϵ^2 (II, 5.51).

Detailed calculations of the differential systems involved for the case $c = 2$, when the outer cylinder is at rest, gave the following new results:

$$\Gamma_{417} = -11{\cdot}858, \quad \Gamma_{4110} = -0{\cdot}0060673, \quad \Gamma_{4111} = 3{\cdot}270 \times 10^{-6}, \quad \Gamma_{4115} = 151{\cdot}06. \tag{3.19}$$

The critical Taylor number to order ϵ^2 is

$$T_c = 1694{\cdot}97 + \epsilon^2(1895{\cdot}8 + 7877{\cdot}1k^2), \tag{3.20}$$

which is close to the value in II(6.10) after correction due to an error in II (see III, p. 110, where 1904 was obtained for the coefficient of ϵ^2 by use of a slide rule, instead of 1895·8). It should also be noted that Γ_{417} is mathematically equivalent to $-\Gamma_2$ in II(5.44). The numerical discrepancy between the value in (3.19) and the value ($-\Gamma_2 = -18{\cdot}16$) given in II(6.9) is due to a numerical error in II. The result concerning the position of maximum vortex activity (II, 6.25) is replaced by

$$\Theta = \tfrac{1}{2}\pi + \epsilon(0{\cdot}487 - 0{\cdot}577k) + O(\delta\epsilon),$$

but the qualitative conclusion following II(6.25) is not affected. In contrast Γ_{418} (see (3.17) with $i = 8$), which is mathematically equivalent to Γ_1 in II(6.8), was chosen to be zero by appropriate choice of the eigenfunction $\mathbf{U}_0$ added to $\mathbf{U}_{211}$, $\mathbf{U}_{212}$ and $\mathbf{U}_{213}$.

Several parameters that were recorded in III(4.30) have been recalculated and the very slightly modified values are as follows:

$$\left.\begin{array}{lll} \lambda = 3{\cdot}127, & T_0 = 1694{\cdot}97, & Q_0 = -0{\cdot}13636, \\ \Gamma = 23{\cdot}088, & \Gamma_3 = 0{\cdot}0073394, & \Gamma_4 = 38{\cdot}154, \\ \Gamma_5 = -2{\cdot}3713, & \Gamma_4' = 40{\cdot}094. & \end{array}\right\} \tag{3.21}$$

Owing to a change in the scale of the adjoint function from III(4.30), Γ_0 is now

$$\Gamma_0 = 0{\cdot}22113. \tag{3.22}$$

The physical interpretation of these results is given in §§ 4 and 5.

We end this section with some remarks on the numerical calculations. Although they were simple enough in principle, the amount of detailed algebra and manipulation was so great that one of the main problems was to devise and carry out suitable checks on the accuracy.

The method of calculation was a simple variant of the 'shooting' method for most of the functions, with a different procedure for the eigenfunction $\mathbf{U}_0$ and for those functions, such as $\mathbf{U}_{211}$, with the same operator as the eigenfunction operator. These methods have been described in Eagles (1971). Many of the same computer routines were employed. All integrations of the differential equations were done using the usual fourth-order Runge–Kutta method, while Simpson's rule was used for the quadratures. Twenty and forty steps were used at various times for checking results.

We list here a number of typical checks made on the results, though the list is not exhaustive.

(i) The eigenfunction $\mathbf{U}_0$ and the adjoint eigenfunction $\mathbf{U}_a$ were checked against those calculated and quoted in II (§ 6).

(ii) In calculating functions such as $\mathbf{U}_{211}$, we used a method (Eagles 1971) which would give the correct zeros in the boundary conditions only if the right-hand side had been correctly calculated. Thus the attainment of the correct zeros was a useful check.

(iii) The parameter Q_0 was checked against the result given in III(4.30).

(iv) We changed the scaling of the eigenfunction $\mathbf{U}_0$ arbitrarily and noted that the consequent changes in magnitude of later functions and constants were consistent.

(v) The functions $\mathbf{U}_{21j}$ ($j = 1, 2, 3$) are arbitrary inasmuch as we may add to each an arbitrary multiple of the eigenfunction $\mathbf{U}_0$. The changes in subsequent functions and constants can be predicted theoretically. It was found that the theoretical changes in, for example, $\mathbf{U}_{301}$, $\mathbf{U}_{302}$, $\mathbf{U}_{304}$, $\mathbf{U}_{321}$, $\mathbf{U}_{322}$, $\mathbf{U}_{324}$ and certain constants Γ_{4ij} were consistent with those found by direct addition of the appropriate eigenfunction multiple in the program. In the final work, we chose to add appropriate multiples of the eigenfunctions to $\mathbf{U}_{2ij}$ ($j = 1, 2, 3$) so that $\Gamma_{418} = \Gamma_{4113} = \Gamma_{4114} = 0$, where these parameters are given by (3.17) with $i = 8$, 13 and 14.

(vi) The identity

$$\Gamma_{417} - \Gamma_{415} = \tfrac{1}{2}\Gamma + \frac{12}{c}\,\Gamma_5 \tag{3.23}$$

and similar identities involving Γ_{4110}, Γ_{4111}, Γ_{4113} and Γ_{4115} were also checked.

(vii) The functions U_0, U_{10}, U_{12}, U_{211}, U_{213}, U_{23}, U_{301}, U_{304}, U_{306}, U_{321} and U_{324} were checked by means of an *independent* theoretical and numerical calculation, which was done in association with the work of DiPrima & Eagles (1977).

(viii) The values of Γ_0, Γ, Γ_4', Γ_5, Γ_3, Γ_4, Γ_{417}, $\Gamma_{415}/\Gamma_{419}$, $\Gamma_{416}/\Gamma_{419}$ and T_c can be inferred from II and III, and the present results agreed after allowing for changes in scaling in relevant cases and for the error in Γ_2 ($= -\Gamma_{417}$) in II.

(ix) Also, it was checked that the physical quantities of interest, the torque and load, were independent of both the normalizations of the basic eigenfunction $\mathbf{U}_0$ and the amount of the eigenfunction included in higher-order functions.

The final results for the constants Γ_i were calculated using 40 steps and are believed to be accurate to four significant figures. The following parameters, which will appear later and are functions of k and T_1, are given in table 1: F_c, F_s, F_{c2}, F_{s2}, σ_1, G_c, G_s, F_1, F_2, F_{X1}, F_{X2}, F_{Y1} and F_{Y2}. They were calculated using 160 steps in $[0, 2\pi]$ and are believed to be accurate to the number of figures quoted.

4. Condition for instability

As mentioned in § 3, the critical value of the Taylor number in the form of (2.1) for $c = 2$, namely

$$T = (q_1 a/\nu)^2 \alpha^3, \tag{4.1}$$

is given by (3.20). Following the argument of II (p. 408), we conclude that the conventional Taylor number

$$T_a = (q_1 a/\nu)^2 \delta^3, \tag{4.2}$$

which contains no factor ϵ, has a critical value

$$T_{ac} = 1695{\cdot}97 + 1969{\cdot}3\delta + 4438{\cdot}3\epsilon^2 + O(\delta^2, \delta\epsilon^2, \epsilon^4), \tag{4.3a}$$

or equivalently

$$T_{ac} = 1694{\cdot}97(1 + 1{\cdot}1618\delta)(1 + 2{\cdot}6185\epsilon^2) + O(\delta^2, \delta\epsilon^2, \epsilon^4). \tag{4.3b}$$

The latter form may be compared with II(6.14) as corrected in III (p. 110). Vohr (1967, 1968) uses a Taylor number $T_v = T_a(1 + \frac{1}{2}\delta)^{-1}$, and the square root of its critical value is

$$T_{vc}^{\frac{1}{2}} = 41{\cdot}17(1 + 0{\cdot}3309\delta)(1 + 1{\cdot}3093\epsilon^2). \tag{4.4}$$

We note that the term proportional to δ in (4.3a, b) and (4.4) arises from $k^2\epsilon^2$ in (3.20) with use of (2.4). Cole (1967, 1969) has noted that, in his experiments, δ (if less than about 0·5) had only a small effect on the ratio of the critical Taylor number to that for $\epsilon = 0$. A similar observation was made by Zarti, Jones & Mobbs (1977) with $\delta < 0{\cdot}43$ approximately and $\epsilon < 0{\cdot}4$ approximately. Our formula (4.3b) is consistent with those observations.

In view of the error in II, figures 2, 3 and 4 in II are in error. Corrected versions are given in this paper as figures 2, 3 and 4. Moreover, reference should be made to figure 2 of Koschmieder (1976), where good agreement is shown for $\epsilon \leqslant 0{\cdot}4$ between his experiments with $\delta = 0{\cdot}375$ and this theory.

Agreement with observation is rather better than appeared to be the case from II. Moreover, Mr Frank Mobbs of the University of Leeds has advised us in conversation that, in figure 4, the data represented by circles, which dip below the value for $\epsilon = 0$, are almost certainly due to what he calls 'trapezoidal' vortices below critical, and are not a manifestation of true Taylor vortices. He has suggested, therefore, that the circled data might be disregarded in comparison with the present theory. We note, however, that similar experimental observations, with a dip below the critical value for $\epsilon = 0$, were reported by Versteegen & Jankowski (1969) and by Frêne & Godet (1971). Furthermore, the relationship of this matter to end effects (Cole 1974a, b, 1976; Jackson & Mobbs 1975; Jackson, Robati & Mobbs 1977; Benjamin 1978a, b; Stuart 1977; and earlier papers cited by Jackson *et al.*) is not at all clear.

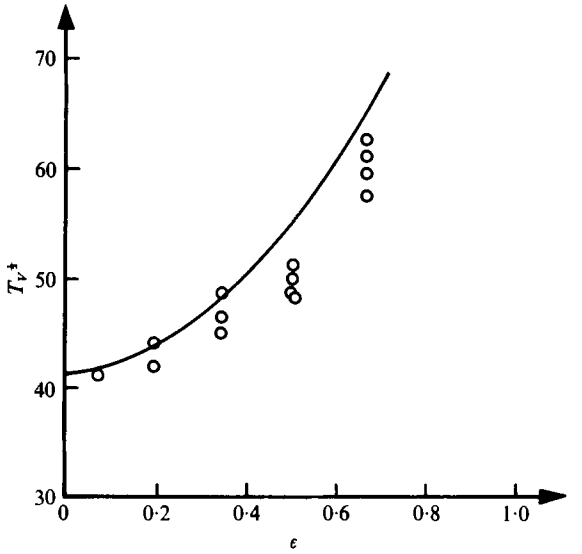

FIGURE 2. Comparison of theory with experimental measurements by Vohr (1968) for $\delta = 0{\cdot}0104$. ——, theory; ○, experiments.

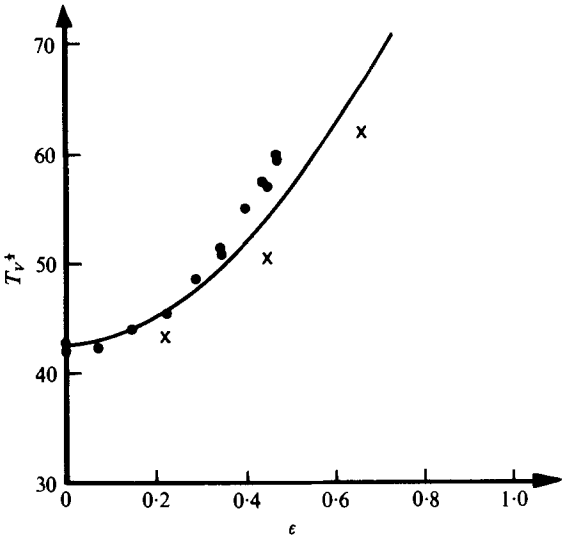

FIGURE 3. Comparison of theory with experimental measurements. ——, theory. Experiments: ●, Vohr (1968) for $\delta = 0{\cdot}099$ using torque measurements; ×, Kamal (1966) for $\delta = 0{\cdot}0904$ using visual observation with aluminium powder.

Recent experimental and theoretical work on the Taylor-vortex and related problems suggests that end effects may destroy the supercritical bifurcation from the two-dimensional basic flow to the three-dimensional Taylor-vortex flow at the critical Taylor number of linearized theory. Rather the end effects immediately introduce very weak Taylor vortices at speeds well below critical which are intensified in the neighbourhood of the critical Taylor number. Some of this work is summarized by Stuart (1977); see also Benjamin (1978*a*, *b*).

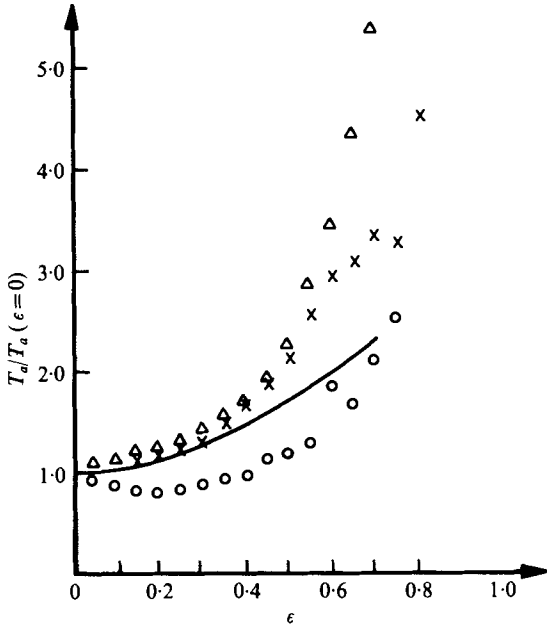

FIGURE 4. Comparison of theory with experimental measurements by Castle & Mobbs (1968) for $\delta = 0{\cdot}112$ (torque) and $\delta = 0{\cdot}0962$ (dye or aluminium). ——, theory. Experiment: ○, first instability (dye); △, second instability (aluminium); ×, second instability (torque).

One further point is that Koschmieder (1976, figure 3) noted a substantial drop in the wavelength in his eccentric-cylinder apparatus for $\epsilon > 0{\cdot}4$, and attributed this to end effects, perhaps because of the relative shortness of his apparatus (at most 25 Taylor vortices long). However, Castle & Mobbs (1968) noticed a substantial drop in wavelength for $\epsilon > 0{\cdot}4$ even in an apparatus 100 vortices long.

5. The flow and pressure fields

The velocity field is obtained by the substitution of (3.1)–(3.4) in (2.6). As explained in § 3, the functions $f, g, h, \ldots$ are given by the solution of inhomogeneous problems of the form typified by (3.11) and (3.12), although the basic eigenvalue problem for $f_0, g_0, h_0, \ldots$ is naturally a homogeneous problem. A complete record of the tables of the functions $\mathbf{U}$ can be obtained from the authors.

The basic structure of the velocity field is clear: at order $\epsilon^{\frac{1}{2}}$ the flow has the same behaviour in x and ξ as in the concentric case through $\mathbf{U}_0(x)$ and $\cos\lambda\xi$, $\sin\lambda\xi$, respectively, but the ϕ variation is given by the multiplicative factor $B(\phi)$. This function is given in III(4.22)–(4.27), in which the constant of integration is chosen to ensure that $B(\phi)$ is 2π-periodic. An associated constant σ_0, defined by III(4.27), is so chosen that

$$\int_0^{2\pi} q_0(\phi)\, d\phi = 0, \tag{5.1}$$

which ensures that the 'lubrication' pressure is 2π-periodic. Thus in (3.2*b*, *d*) the

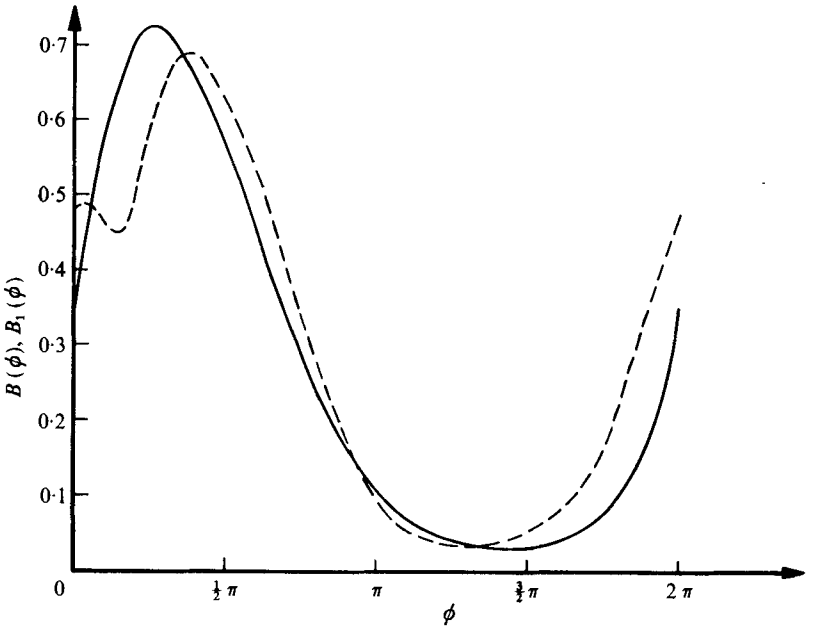

FIGURE 5. The variation of $B(\phi)$ and $B_1(\phi)$ with ϕ for $k = 0{\cdot}31$ and $T_1 = 700$. ——, $B(\phi)$; – – –, $B_1(\phi)$.

value $\sigma_0 = 6Q_0\Gamma_3 T_1/\Gamma_4$ has been used in the terms independent of $B^2(\phi)$. An example of $B^2(\phi)$ is given in III (figure 2) and is repeated here in figure 5 as $B(\phi)$.

Just as in II, on the linearized problem, an additional function $B_1(\phi)$, which multiplies the eigenfunction, is introduced at order $\epsilon^{\frac{3}{2}}$. The differential equation governing $B_1(\phi)$ is given by (3.14), where the Γ parameters are displayed in (3.19) and (3.21) and σ_1 is given by (3.15) and (3.16). The arbitrary constant of integration in (3.14) is determined by the need for $B_1(\phi)$ to be 2π-periodic. The numbers k and T_1 must be chosen to reflect the particular conditions in the experiment, namely the ratio $\delta^{\frac{1}{2}}/\epsilon$ and the elevation ϵT_1 of the Taylor number above its critical value.

Graphs of $B(\phi)$ and $B_1(\phi)$ for $k = 0{\cdot}31$ and $T_1 = 700$ are given in figure 5. The values of k and T_1 have been chosen to relate to observations of Vohr (1968) with $\delta = 0{\cdot}099$ and $\epsilon = 0{\cdot}475$ (III, p. 101). At a Taylor-number elevation ϵT_1 above critical of some 20 % when the outer cylinder was at rest, the maximum Taylor-vortex strength observed visually was at 50° downstream of maximum gap. Although δ and ϵ are rather large for the application of the present theory, it is of interest to make the appropriate calculations.

As in II (p. 412) we choose to make a comparison with $\partial w/\partial x$ at the outer cylinder and, since the dominant term of the expression is strongest at $\lambda\xi = \frac{1}{2}\pi$, we restrict ourselves to that value. The expression for w is given by (2.6), (3.1), (3.2c), (3.3c) and (3.4c) with $\lambda\xi = \frac{1}{2}\pi$, and its x derivative has the form

$$\partial w(\tfrac{1}{2}, \phi, \pi/2\lambda)/\partial x = \epsilon^{\frac{1}{2}} B(\phi)\, s_0(\tfrac{1}{2}) + \epsilon^{\frac{3}{2}}\{B_1(\phi)\, s_0(\tfrac{1}{2}) + T_1 B(\phi)\, s_{211}(\tfrac{1}{2}) + B(\phi)\cos\phi\, s_{212}(\tfrac{1}{2}) + B^3(\phi)\,[s_{213}(\tfrac{1}{2}) - s_{23}(\tfrac{1}{2})]\} + O(\epsilon^{\frac{5}{2}}). \quad (5.2)$$

We need the location ϕ_M of the maximum as ϕ varies. For small ϵ we write

$$\phi_M = \phi_{M0} + \epsilon\phi_{M1}, \tag{5.3}$$

where ϕ_{M0} satisfies $dB/d\phi = 0$ and

$$\phi_{M1} = -\frac{kT_0^{\frac{1}{2}}}{\Gamma}\left[\frac{S_{212}(\frac{1}{2})}{S_0(\frac{1}{2})} - \frac{dB_1(\phi_{M0})/d\phi}{B(\phi_{M0})\sin\phi_{M0}}\right]. \tag{5.4}$$

In addition, we need to bear in mind that ϕ is not the physical angle Θ measured on the outer cylinder; however, using the formulae of II (p. 411), we find that, to order ϵ, the angle Θ_M for maximum Taylor-vortex activity is given by

$$\Theta_M = \phi_{M0} + \epsilon(\phi_{M1} + \sin\phi_{M0}). \tag{5.5}$$

For the values of k and T_1 quoted, we find numerically that

$$\phi_{M0} = 0{\cdot}821, \quad \phi_{M1} = -0{\cdot}676, \tag{5.6}$$

from which, for $\epsilon = 0{\cdot}475$, we obtain

$$\phi_M = 0{\cdot}500, \quad \Theta_M = 0{\cdot}848. \tag{5.7}$$

In (5.3) the ratio of the second term to the first is rather large, being 0·39, but in (5.5) the corresponding ratio is 0·03. The upshot is that the angle Θ_M is about 49°, which is very close to Vohr's observation. In contrast, we note (III, pp. 101–102) that, when ϕ_{M1} is ignored as in III, we have $\phi_M = 47°$ and $\Theta_M = 67°$. [Note that the disparity between $\Theta = 76°$ in III (p. 101) and $\Theta = 67°$ arises from an ϵ^2 effect in use of the complete formula II(6.18) instead of (5.5).] Thus the effect of ϕ_{M1}, which is an order-ϵ correction due to the flow, is essentially to cancel the difference between ϕ_M and Θ_M.

Bearing in mind that Dr Vohr has told us that his observation was 'certainly qualitative and subjective' and that 'reattachment, following separation, may have affected the observations' (III, pp. 101–102), we believe that the present theory has shown that it is capable of explaining the substantial shift of the maximum vortex strength downstream from the maximum gap. We note, however, that Koschmieder (1976), in an eccentric-cylinder apparatus with $\delta = 0{\cdot}375$ and for the two values $\epsilon = 0{\cdot}278$ and 0·556, reports being unable to see a location of maximum Taylor-vortex activity. Clearly more work is required on this type of comparison, and we understand from Mr Frank Mobbs that such work is in progress at the University of Leeds.

We turn now to the kinematic pressure field for the case when the outer cylinder is at rest ($c = 2$). From (2.1), (2.4), (2.5) and (2.7), we obtain

$$p'(x,\phi,\xi,\tau) = (\nu q_1/a\alpha^2)[P(x,\phi) + p_R(\phi)] + (\nu^2/a^2\alpha^2)[\epsilon^{\frac{1}{2}} p_0(x,\phi,\xi) + O(\epsilon)], \tag{5.8}$$

where we have converted the 'lubrication' part of the perturbation pressure field, namely the part proportional to

$$p_R(\phi) = \epsilon\int_0^\phi q_0(\phi)\,d\phi + \epsilon^2\int_0^\phi q_1(\phi)\,d\phi + O(\epsilon^2), \tag{5.9}$$

to have the Reynolds scaling of lubrication theory. The ratio of this part of (5.8) to the 'usual' Taylor-vortex pressure field $p_0(x,\phi,\xi)$ is still $O(\epsilon^{-\frac{1}{2}})$.

Vohr (1967) has made measurements of the pressure field on the outer cylinder for the cases $\delta = 0{\cdot}0104$ with $\epsilon = 0{\cdot}2$, 0·35, 0·51 and 0·68. Although his data are for a

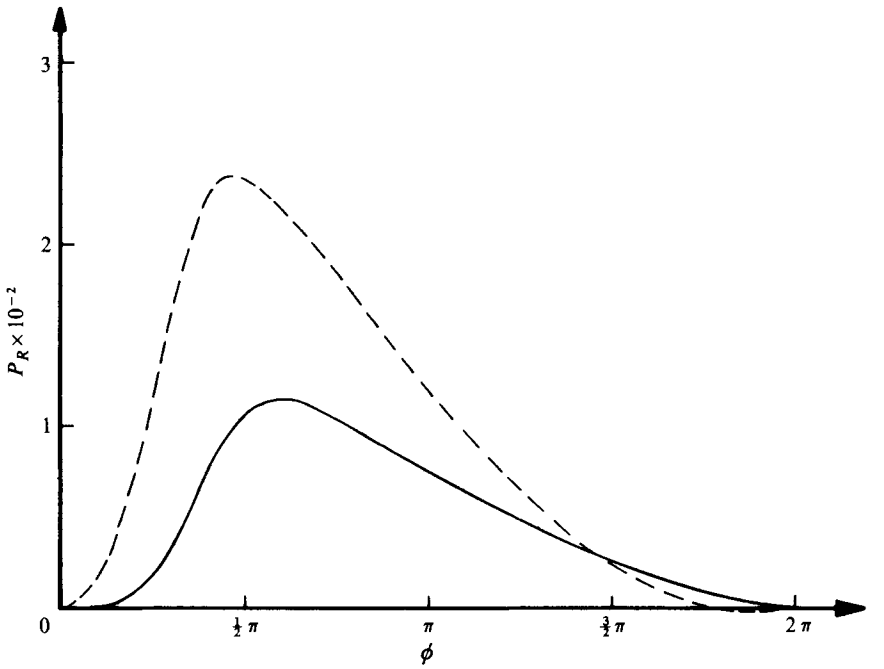

FIGURE 6. The variation of $p_R(\phi)$ with ϕ for $\epsilon = 0{\cdot}2$, $\delta = 0{\cdot}0104$ ($k = 0{\cdot}253$). ——, $T_a = 1{\cdot}01T_{ac}$; —, $T_a = 1{\cdot}03T_{ac}$.

much higher Taylor number than the present theory (or perhaps any perturbation theory) can hope to reach, it is nevertheless of some interest to evaluate the two parts of (5.9). Since our theory requires ϵ to be small, we restrict ourselves to the case $\epsilon = 0{\cdot}2$, which is the lowest value for which Vohr (1967) quotes measurements. The corresponding value of k is 0·253.

In figure 6 we show $p_R(\phi)$ plotted against ϕ for Taylor-number elevations 1 % and 3 % above critical. In the former case, the ratio of the second to the first term in (5.9) is about $\frac{2}{5}$, while in the latter example the ratio is about $\frac{1}{2}$. Even for such low Taylor-number elevations, therefore, it is seen that the perturbation theory is at the limits of its applicability, at least as far as the pressure is concerned. Moreover, for an elevation 10 % above critical, the ratio of the two terms in (5.9) is so high ($\frac{3}{2}$) as to render application of the theory pointless.

It is known from I (equation 91) that $P(x, \phi)$ is of order 1 when $\epsilon = 0{\cdot}2$, so that our result for $p_R(\phi)$ is only 1–3 % of the laminar pressure. In view of the fact that Vohr's experiments were conducted at a Taylor number of order ten times the critical value, we do not pursue this comparison further, except to note that, in contrast to figure 6, his measurements (Vohr 1967, figures 19, 20) suggest a pressure function p_R anti-symmetric about $\Theta = \phi = \pi$. This may be a strongly nonlinear effect, which the present weakly nonlinear theory cannot treat.

6. The torque and load

The basic formulae for the torque and load acting on the inner cylinder are given in III (p. 103). After a large amount of work, we find the following expressions for the torque T_i and the loads F_X and F_Y in the X and Y directions of figure 1:

$$\left.\begin{aligned} T_i &= (-2\pi\mu q_1 la/\delta)(G_B+G_{TV}),\\ G_B &= 1+2\epsilon^2+\tfrac{3}{2}\delta+O(\epsilon^4,R_m^2), \quad G_{TV}=(-\epsilon/2\pi)[G_1(T_1)+\epsilon G_2(k,T_1)+O(\epsilon^2)],\end{aligned}\right\} \tag{6.1}$$

$$\left.\begin{aligned} F_X &= (-\pi\mu q_1 l/\delta^2)(F_{XB}+F_{XTV}),\\ F_{XB} &= \tfrac{1}{3}R_m\epsilon[1+O(\epsilon^2)], \quad F_{XTV}=(\epsilon/\pi)[F_{X1}(k,T_1)+\epsilon F_{X2}(k,T_1)+O(\epsilon^2)],\end{aligned}\right\} \tag{6.2}$$

$$\left.\begin{aligned} F_Y &= (-\pi\mu q_1 l/\delta^2)(F_{YB}+F_{YTV}),\\ F_{YB} &= 6\epsilon[1+\tfrac{1}{2}\delta+O(\epsilon^3)], \quad F_{YTV}=(\epsilon/\pi)[F_{Y1}(k,T_1)+\epsilon F_{Y2}(k,T_1)+O(\epsilon^2)].\end{aligned}\right\} \tag{6.3}$$

In these formulae, the terms G_B, F_{XB} and F_{YB} represent the contributions of the basic flow and the terms G_{TV}, F_{XTV} and F_{YTV} the contributions due to the Taylor vortices. The notation is the same as in III(6.8)–(6.10) except that a factor 6 that appears in the scale factor for F_Y in III has been placed in F_{YB} and F_{YTV}. The following relations are valid for (6.1)–(6.3):

$$G_1(T_1) = G_{10}T_1, \tag{6.4}$$

$$G_2(k,T_1) = G_{20}T_1^2+G_{21}F_c(k,T_1), \tag{6.5}$$

$$F_{X1}(k,T_1) = 6Q_0F_s(k,T_1), \tag{6.6}$$

$$F_{X2}(k,T_1) = F_{X20}kF_c(k,T_1)+F_{X21}T_1F_s(k,T_1)+F_{X22}F_{s2}(k,T_1)+12Q_0G_s(k,T_1), \tag{6.7}$$

$$F_{Y1}(k,T_1) = -6Q_0F_c(k,T_1), \tag{6.8}$$

$$\begin{aligned} F_{Y2}(k,T_1) = {} & F_{Y20}T_1+F_{Y21}T_1F_c(k,T_1)+F_{Y22}kF_s(k,T_1)+F_{Y23}F_{c2}(k,T_1)\\ & -12Q_0G_c(k,T_1), \end{aligned} \tag{6.9}$$

where Q_0 is given by (3.21) and the other coefficients are

$$\left.\begin{aligned} G_{10} &= -5{\cdot}666\times10^{-3}, \quad G_{20}=5{\cdot}284\times10^{-6}, \quad G_{21}=12{\cdot}30,\\ F_{X20} &= F_{Y22}=6{\cdot}970, \quad F_{X21}=-F_{Y21}=2{\cdot}461\times10^{-3},\\ F_{X22} &= -F_{Y23}=1{\cdot}321, \quad F_{Y20}=-1{\cdot}102\times10^{-3}.\end{aligned}\right\} \tag{6.10}$$

In addition, $F_c(k,T_1)$ and $F_s(k,T_1)$ are given by III(6.11) and

$$F_{c2}(k,T_1) = \int_0^{2\pi}B^2(\phi)\cos2\phi\,d\phi, \quad F_{s2}(k,T_1) = \int_0^{2\pi}B^2(\phi)\sin2\phi\,d\phi, \tag{6.11}$$

$$G_c(k,T_1) = \int_0^{2\pi}B(\phi)B_1(\phi)\cos\phi\,d\phi, \quad G_s(k,T_1) = \int_0^{2\pi}B(\phi)B_1(\phi)\sin\phi\,d\phi. \tag{6.12}$$

Since $B(\phi)$ and $B_1(\phi)$ follow from integration of III(4.22)–(4.27) and of (3.14), with the numerical coefficients known from (3.19) and (3.21), formulae (6.1)–(6.14) give sufficient information for the calculation of the torque and load for any values of the parameters within the range of applicability of the theory.

T_1	F_c	F_s	F_{c2}	F_{s2}	σ_1	G_c	G_s	F_1	F_2	F_{X_1}	F_{X_2}	F_{Y_1}	F_{Y_2}
					(*a*) $\epsilon = 0{\cdot}02$, $k = 2{\cdot}549$, $T_{ac} = 1717{\cdot}22$								
858·6	0·02739	0·2196	−0·0228	0·00727	0·5307	−0·0072	−0·1124	−4·865	4·232	−0·1797	1·144	0·0224	2·916
2575·8	0·2201	0·5880	−0·0393	0·0493	4·754	−0·3066	−0·9066	−14·60	37·77	−0·4810	9·185	0·1801	5·762
4293·0	0·5033	0·8063	−0·0132	0·0830	13·11	−1·217	−2·083	−24·33	103·6	−0·6597	20·98	0·4118	2·302
8586·1	1·100	0·8793	0·0571	0·0582	51·64	−5·450	−4·599	−48·65	403·1	−0·7194	45·73	0·9002	−26·08
12879	1·409	0·7488	0·0582	0·0134	115·3	−10·55	−5·938	−72·98	893·8	−0·6126	58·49	1·152	−62·88
17172	1·561	0·6212	0·0420	−0·0058	204·1	−15·68	−6·627	−97·30	1577·4	−0·5082	64·81	1·277	−99·55
					(*b*) $\epsilon = 0{\cdot}04$, $k = 1{\cdot}274$, $T_{ac} = 1722{\cdot}53$								
430·6	0·0250	0·2066	−0·0421	0·0128	0·1494	0·00348	−0·0639	−2·440	1·288	−0·1690	0·5627	0·0205	1·395
1291·9	0·2034	0·5590	−0·0763	0·0892	1·325	−0·1574	−0·5083	−7·320	11·32	−0·4574	4·533	0·1664	2·737
2153·2	0·4730	0·7785	−0·0323	0·1559	3·601	−0·6649	−1·140	−12·20	30·31	−0·6370	10·40	0·3870	0·9881
4306·3	1·071	0·8743	0·1068	0·1195	13·69	−2·904	−2·363	−24·40	111·2	−0·7154	22·80	0·8759	−13·22
6459·5	1·393	0·7519	0·1154	0·0307	29·90	−5·453	−2·957	−36·60	237·6	−0·6152	29·20	1·140	−31·66
8612·6	1·553	0·6247	0·0846	−0·0098	52·35	−7·977	−3·271	−48·80	411·1	−0·5111	32·37	1·271	−50·03
					(*c*) $\epsilon = 0{\cdot}08$, $k = 0{\cdot}636$, $T_{ac} = 1743{\cdot}76$								
218·0	0·0190	0·1708	−0·0648	0·0173	0·0493	0·0125	−0·0392	−1·235	0·4847	−0·1397	0·2629	0·0155	0·6126
653·9	0·1584	0·4742	−0·1329	0·1279	0·4326	−0·0674	−0·3128	−3·705	4·207	−0·3879	2·416	0·1296	1·192
1089·9	0·3838	0·6878	−0·0885	0·2472	1·153	−0·3706	−0·6983	−6·175	11·00	−0·5628	5·015	0·3140	0·3291
2179·7	0·9632	0·8489	0·1598	0·2512	4·109	−1·718	−1·331	−12·35	36·95	−0·6945	11·33	0·7880	−6·829
3269·6	1·329	0·7609	0·2189	0·0892	8·512	−3·065	−1·495	−18·53	72·83	−0·6226	14·58	1·087	−16·23
4359·4	1·521	0·6378	0·1725	−0·0050	14·40	−4·279	−1·569	−24·70	119·1	−0·5218	16·15	1·245	−25·53
					(*d*) $\epsilon = 0{\cdot}2$, $k = 0{\cdot}253$, $T_{ac} = 1892{\cdot}63$								
94·63	0·0092	0·0999	−0·0674	0·0135	0·0142	0·0159	−0·0175	−0·5362	0·1599	−0·0817	0·0859	0·0075	0·1847
283·9	0·0783	0·2873	−0·1659	0·1079	0·1239	0·0070	−0·1452	−1·609	1·388	−0·2350	0·7189	0·0640	0·3694
473·2	0·1991	0·4439	−0·1849	0·2441	0·3282	−0·0999	−0·3466	−2·681	3·631	−0·3632	1·758	0·1629	0·1101
946·3	0·5967	0·6774	0·0290	0·4607	1·138	−0·7818	−0·7926	−5·362	12·07	−0·5542	4·535	0·4882	−2·556
1419·5	0·9856	0·7307	0·2816	0·3870	2·248	−1·677	−0·8917	−8·043	22·77	−0·5978	6·261	0·8064	−6·836
1892·7	1·288	0·6794	0·3722	0·1866	3·590	−2·420	−0·7446	−10·72	34·77	−0·5558	6·900	1·054	−11·34
					(*e*) $\epsilon = 0{\cdot}35$, $k = 0{\cdot}141$, $T_{ac} = 2257{\cdot}84$								
64·51	0·0065	0·0725	−0·0584	0·0109	0·0085	0·0141	−0·0118	−0·3655	0·1013	−0·0593	0·0517	0·0053	0·0994
193·5	0·0548	0·2097	−0·1488	0·0879	0·0737	0·0165	−0·0979	−1·097	0·8715	−0·1716	0·4300	0·0448	0·1902
322·5	0·1385	0·3284	−0·1827	0·2031	0·1928	−0·0424	−0·2346	−1·828	2·253	−0·2687	1·049	0·1133	0·0291
645·1	0·4217	0·5337	−0·0626	0·4483	0·6553	−0·4593	−0·5768	−3·655	7·384	−0·4367	2·798	0·3450	−1·525

TABLE 1. Values of different constants for various values of ϵ and T_1 for $\delta = 0{\cdot}0104$. The lines correspond to 1, 3, 5, 10, 15 and 20 % above $T_c(\epsilon)$. The elevation above $T_{ac}(\epsilon)$ is slightly different for the larger values of ϵ. For $\epsilon = 0{\cdot}35$ results are given only up to 10 % above critical.

$T_a^{\frac{1}{2}}$	T_1	G_{TV}	F_{XTV}	F_{YTV}
	(*a*) $\epsilon = 0{\cdot}02$, $k = 2{\cdot}549$, $T_{ac} = 1717{\cdot}22$, $T_{ac}^{\frac{1}{2}} = 41{\cdot}44$			
41·64	858·6	0·0152	−0·0010	0·0005
42·06	2575·8	0·0441	−0·0019	0·0019
42·45	4293·0	0·0708	−0·0015	0·0029
43·46	8586·1	0·1292	0·0012	0·0024
44·44	12879	0·1754	0·0035	−0·0007
45·40	17172	0·2093	0·0050	−0·0045
	(*b*) $\epsilon = 0{\cdot}04$, $k = 1{\cdot}274$, $T_{ac} = 1722{\cdot}53$, $T_{ac}^{\frac{1}{2}} = 41{\cdot}50$			
41·71	430·6	0·0152	−0·0019	0·0010
42·12	1291·9	0·0437	−0·0035	0·0035
42·53	2153·2	0·0699	−0·0028	0·0054
43·53	4306·3	0·1270	0·0025	0·0044
44·51	6459·5	0·1725	0·0070	−0·0016
45·47	8612·6	0·2060	0·0100	−0·0093
	(*c*) $\epsilon = 0{\cdot}08$, $k = 0{\cdot}636$, $T_{ac} = 1743{\cdot}76$, $T_{ac}^{\frac{1}{2}} = 41{\cdot}76$			
41·97	218·0	0·0152	−0·0030	0·0016
42·39	653·9	0·0429	−0·0055	0·0057
42·80	1089 9	0·0674	−0·0041	0·0087
43·82	2179·7	0·1196	0·0054	0·0062
44·81	3269·6	0·1617	0·0138	−0·0054
45·78	4359·4	0·1932	0·0196	−0·0203
	(*d*) $\epsilon = 0{\cdot}2$, $k = 0{\cdot}253$, $T_{ac} = 1892{\cdot}63$, $T_{ac}^{\frac{1}{2}} = 43{\cdot}50$			
43·74	94·63	0·0160	−0·0041	0·0028
44·19	283·9	0·0424	−0·0058	0·0088
44·65	473·2	0·0622	−0·0007	0·0118
45·76	946·3	0·0938	0·0225	−0·0015
46·84	1419·5	0·1111	0·0417	−0·0357
47·91	1892·7	0·1199	0·0525	−0·0773
	(*e*) $\epsilon = 0{\cdot}35$, $k = 0{\cdot}141$, $T_{ac} = 2257{\cdot}84$, $T_{ac}^{\frac{1}{2}} = 47{\cdot}52$			
47·80	64·51	0·0184	−0·0046	0·0045
48·38	193·5	0·0441	−0·0024	0·0124
48·94	322·5	0·0579	0·0110	0·0138
50·32	645·1	0·0596	0·0605	−0·0210

TABLE 2. Torque and loads for $\delta = 0{\cdot}0104$ for various values of ϵ and T_1.

For this paper, detailed calculations have been made of the torque and load for a set of values of ϵ with $\delta = 0{\cdot}0104$, as in Vohr's (1967, 1968) experiments, and for several values of the elevation of the Taylor number T_a above critical up to about 20 %. The values of ϵ chosen initially were 0·20 and 0·35, the lowest values in the experiments; later, because of doubts over the validity of the series at such relatively large values of ϵ, we did calculations also for $\epsilon = 0{\cdot}02$, 0·04 and 0·08. The results are given in tables 1 (*a*)–(*e*). At the head of each table we give the value of k defined by (2.4) and the critical Taylor number in the form T_{ac} defined by (4.3*a*).

In tables 2 (*a*)–(*e*) we give the functions G_{TV}, F_{XTV} and F_{YTV} defined in (6.2), (6.3) and (6.4), so that direct comparison can be made with calculations recorded in III (table 3). It should be noted that the relevant Taylor number for table 2 is T_a. Thus the elevation of the Taylor number above critical is not ϵT_1 but $\epsilon T_1(1-\epsilon^2)^{-\frac{1}{2}}$, where

ϵ	G_{TV} (%)	F_{XTV} (%)	F_{YTV}
0·02	20	3	?
0·04	20	3	?
0·08	20	3	?
0·20	10	1	?
0·35	6	1	?

TABLE 3. Suggested range of validity of Taylor-vortex torque and load calculations as a percentage of the Taylor-number elevation above the critical value of $T_a(\epsilon)$ for $\delta = 0{\cdot}0104$ and a range of values of ϵ.

the multiplicative factor arises in going from T to T_a. A few words of caution are necessary about the range of validity of the perturbation scheme. We have taken as a rough criterion that results for the torque and load are acceptable if the second term in the perturbation is less than one-half of the first, a very optimistic view indeed. From this criterion we obtain the tentative ranges of validity shown in table 3 for the results on the torque and load given in table 2. The estimates in table 3 are approximate and based on only the data at the intervals in table 1. Whereas the torque and similarly F_X, at least for a small elevation above critical, are predicted reasonably well, there are grave doubts about F_Y. Some analytical reasoning will now be given by way of explanation of this difficulty with the present perturbation analysis. It is necessary to transform the solutions into series in powers of the Taylor-number elevation above critical.

It is known (II, p. 413) that if $k \to \infty$ (T_1 fixed) we retrieve the solution for the linearized concentric case. [We know also from III (p. 100) that the nonlinear concentric case can be retrieved from the limit $T_1 \to \infty$ (k fixed), but we do not pursue that possibility here.] In the present work we extend to the nonlinear case the idea of $k \to \infty$ (T_1 fixed) being an appropriate limit for the concentric problem. At the same time, we shall produce an expansion in powers of Taylor-number elevation above the critical value. After much labour, we find forms for the functions G_{TV}, F_{XTV} and F_{YTV} of (6.1)–(6.3) as follows, where T_1 has been eliminated by use of $T_1 = \epsilon^{-1}(T - T_c)$:

$$G_{TV} = -(2\pi)^{-1}\{G_{10}(T-T_c) + (T-T_c)^2[G_{20} + G_{21}(g_{c1}k^2 + g_{c2}k^{-4})]\}, \tag{6.13}$$

$$F_{XTV} = (a_1^{(1)}k^{-1} + a_1^{(3)}k^{-3} + \ldots)(T-T_c) + (a_2^{(1)}k^{-1} + a_2^{(3)}k^{-3} + \ldots)(T-T_c)^2 + O(T-T_c)^3, \tag{6.14}$$

$$F_{YTV} = \epsilon(b_1^{(0)} + b_1^{(2)}k^{-2})(T-T_c) + \alpha^{-\frac{1}{2}}(b_2^{(1)}k^{-1} + b_2^{(3)}k^{-3})(T-T_c)^2 + O(T-T_c)^3. \tag{6.15}$$

In these formulae the g's, a's and b's are pure numbers. It is worth noting that in (6.13) letting $k \to \infty$ with $T - T_c$ fixed gives the same numerical values for the torque in the concentric case as were reported by DiPrima & Eagles (1977).

In (6.13) and (6.14) the terms proportional to $T - T_c$ come from the corresponding terms $O(\epsilon)$ in (6.1) and (6.2), while the terms which are proportional to $(T - T_c)^2$ come from the terms $O(\epsilon^2)$ in (6.1) and (6.2). In view of the fact that ϵT_1 is proportional to $T - T_c$ this seems perfectly natural. Bearing this in mind, we turn to (6.15); here the term proportional to $T - T_c$ arises from the $O(\epsilon^2)$ term in (6.3), while the term $(T - T_c)^2$

arises from the $O(\epsilon)$ term in (6.3). Thus the ordering which is felt to be natural is reversed! This arises as a consequence of the fact that F_{Y2} in (6.9) is proportional to T_1 as $k \to \infty$, while F_{Y1} in (6.8) is proportional to T_1^2 as $k \to \infty$.

The upshot of these remarks is the observation that our expansion disorders the 'natural' form of expansion in powers of $T - T_c$ for the Taylor-vortex contribution to F_Y. We believe that this is basically the reason why the $O(\epsilon)$ and $O(\epsilon^2)$ terms in the original expansion are of comparable magnitude; and for this reason we have questioned in table 3 the validity of the results for F_{YTV} given in table 2. These remarks should not be interpreted to mean that the results are incorrect, but rather that we cannot assert their validity on the basis of the usual rules of perturbation theory. This deficiency could perhaps be remedied by means of a direct expansion of the Taylor-vortex flow in powers of $T - T_c$.

As far as the torque is concerned, we have not compared our results with Vohr's torque figures nor with the torque figures given by Castle & Mobbs (1968) and Castle, Mobbs & Markho (1971) since the present work does not go to high-enough order to give the δ and ϵ^2 corrections to the coefficients of $T - T_c$ in (6.13). This would be necessary to make thoroughly effective comparisons, but would require a calculation of the torque to order ϵ^3 in our expansions, whereas the present calculation goes to order ϵ^2.

However, we note that Vohr (1967) has shown experimentally that, in a plot of dimensional torque against speed, the angle of bifurcation, between the torque curves for laminar and for Taylor-vortex flow, decreases as ϵ increases. Cole (1967, 1969) observed a similar phenomenon in a series of experiments for different values of δ, and the papers of Castle & Mobbs (1968), Castle *et al.* (1971) and Markho, Jones & Mobbs (1977) also give some support to Vohr's observation. Our theory does not go to a high-enough order to show this explicitly since, as can be seen from (6.13), the coefficient of $T - T_c$ is independent of ϵ to order ϵ^2. On the other hand, Vohr's observations seem also to be consistent with the idea that the additional torque due to Taylor vortices drops as ϵ increases, with the percentage elevation of the Taylor number above critical held fixed.

In order to eliminate the effect of speed and to obtain results qualitatively comparable with Vohr's dimensional data in units of inch pounds, we have rewritten the Taylor-vortex part of (6.1) as

$$(T_i)_{TV} = -l\mu\nu\delta^{-\frac{1}{2}}T_0^{\frac{1}{2}}\Delta, \tag{6.16}$$

$$\Delta = -\epsilon G_1(T_1) - \epsilon^2[G_2(k, T_1) + (T_1/2T_0)\, G_1(T_1)]. \tag{6.17}$$

Figure 7 shows Δ plotted against $T_a^{\frac{1}{2}}$ for several values of ϵ. The dashed curve shows the torque at a T_a value 5 % above the ϵ-dependent critical value, and indeed shows a fall in the torque, albeit slight. More extensive calculations would be needed to take this comparison further.

Finally, accepting for the moment the results given in table 2, we observe that the Taylor-vortex corrections to the basic load are smaller than those to the basic torque. For example, for $\delta = 0{\cdot}0104$, $\epsilon = 0{\cdot}04$ and $T_a^{\frac{1}{2}} = 43{\cdot}53$, which is an elevation of T_a above its critical value of 10 %, we find from table 2 and (6.1)–(6.3) that

$$G_{TV}/G_B \sim 0{\cdot}12, \quad F_{YTV}/F_{YTB} \sim 0{\cdot}02 \quad \text{and} \quad |F_{XTV}/F_{XB}| \sim 0{\cdot}07.$$

This is consistent with the related experiments of Frêne & Godet (1974) on a loaded

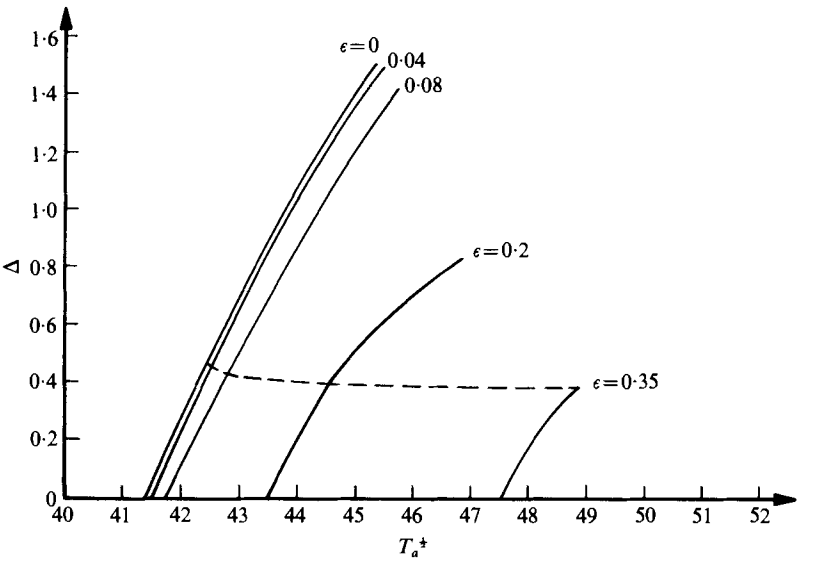

FIGURE 7. The dimensionless excess torque Δ above the torque for circular Couette flow as a function of $T_a^{\frac{1}{2}}$ for ϵ equal to 0, 0·04, 0·08, 0·2, 0·35. The dashed curve shows the torque at 5% above the critical value of T_a for the different values of ϵ.

journal bearing. They observed 'no significant differences between the load carrying capacity of bearings operating in the laminar or in the vortex flow regions. Beyond the transition point, friction torque is sizeably increased ...'.

7. Concluding remarks

The work described in this paper has taken to higher order in ϵ the nonlinear calculation described in III. The results of this paper are as follows.

(i) The calculated angle at which the Taylor-vortex activity is predicted to be strongest is some 49° downstream of the maximum gap, in excellent agreement with Vohr's observations in spite of the experimental conditions being somewhat outside the range of validity of the theory.

(ii) At a given percentage elevation of the Taylor number above critical, the additional torque due to Taylor vortices drops slightly as ϵ increases, qualitatively in accordance with experiment.

(iii) Formulae have been given for the torque and load on the inner cylinder. As far as the torque is concerned, the present theory is believed to be reasonably accurate for a range of eccentricities and Taylor numbers, but the accuracy is less acceptable for the component of the load in the X direction. Moreover, for the component of the load in the Y direction, the order-ϵ and order-ϵ^2 terms appear to be comparable in magnitude, a feature which we associate with a disordering of the terms in the expansion for the Y component of the load, but *not* in the expansions for the X component and the torque. The only observations of the torque and load known to the authors were made at too high a Taylor number (ten times the critical value) for the theory to have any accuracy.

We conclude that further theoretical and experimental work is needed on the

problem, in order to bring results closer to a reasonable comparison. From a theoretical point of view, this might be achieved by an expansion in $T - T_c$ with ϵ and δ kept fixed, but then a formidable set of calculations would be required.

Much of this work was done while J. T. Stuart was visiting Rensselaer Polytechnic Institute or R. C. DiPrima was a visitor at Imperial College. It was supported in part by the Office of Naval Research, the Army Research Office, the Science Research Council of Great Britain, and by a NATO Research Grant for travel. The calculations were carried out at the City University of London, and thanks are extended to the staff of the Computing Centre. Also, we wish to thank Mr Frank Mobbs of the University of Leeds for helpful advice about the experiments of himself and his colleagues.

REFERENCES

BENJAMIN, T. B. 1978*a* Bifurcation phenomena in steady flow of a viscous liquid. Part 1. Theory. *Proc. Roy. Soc.* A **359**, 1–26.

BENJAMIN, T. B. 1978*b* Bifurcation phenomena in steady flow of a viscous liquid. Part 2. Experiments. *Proe. Roy. Soc.* A **359**, 27–43.

BENNEY, D. J. & ROSKES, G. J. 1969 Wave instabilities. *Stud. Appl. Math.* **48**, 377–385.

CASTLE, P. & MOBBS, F. S. 1968 Hydrodynamic stability of the flow between eccentric rotating cylinders: visual observations and torque measurements. *Proc. Inst. Mech. Engrs* **182** (3N), 41–52.

CASTLE, P., MOBBS, F. R. & MARKHO, P. H. 1971 Visual observations and torque measurements in the Taylor-vortex regime between eccentric rotating cylinders. *Trans. A.S.M.E., J. Lub. Tech.* F **93**, 121–129.

COLE, J. A.. 1967 Taylor vortices with eccentric rotating cylinders. *Nature* **216**, 1200–1202.

COLE, J. A.. 1969 Taylor vortices with eccentric rotating cylinders. *Nature* **221**, 253–254.

COLE, J. A. 1974*a* Taylor vortices with short rotating cylinders. *J. Fluids Engng* **96**, 69–70.

COLE, J. A. 1974*b* Taylor vortex behaviour in annular clearances of limited length. *Proc. 5th Austr. Conf. Hydraul. Fluid Mech.* pp. 514–521.

COLE, J. A. 1976 Taylor-vortex instability and annulus-length effects. *J. Fluid Mech.* **75**, 1–15.

DAVEY, A. 1962 The growth of Taylor vortices in flow between rotating cylinders. *J. Fluid Mech.* **14**, 336–368.

DAVEY, A., HOCKING, L. M. & STEWARTSON, K. 1974 On the nonlinear evolution of three-dimensional disturbances in plane Poiseuille flow. *J. Fluid Mech.* **63**, 529–536.

DAVEY, A. & STEWARTSON, K. 1974 On three-dimensional packets of surface waves. *Proc. Roy. Soc.* A **338**, 101–110.

DIPRIMA, R. C. & EAGLES, P. M. 1977 Amplification rates and torques for Taylor-vortex flows between rotating cylinders. *Phys. Fluids* **20**, 171–175.

DIPRIMA, R. C. & STUART, J. T. 1972*a* Flow between eccentric rotating cylinders. *Trans. A.S.M.E., J. Lub. Tech.* F **94**, 266–274.

DIPRIMA, R. C. & STUART, J. T. 1972*b* Non-local effects in the stability of flow between eccentric rotating cylinders. *J. Fluid Mech.* **54**, 393–415.

DIPRIMA, R. C. & STUART, J. T. 1974 Development and effects of supercritical Taylor-vortex flow in a lightly-loaded journal bearing. *Trans. A.S.M.E., J. Lub. Tech.* F **94**, 28–35.

DIPRIMA, R. C. & STUART, J. T. 1975 The nonlinear calculation of Taylor-vortex flow between eccentric rotating cylinders. *J. Fluid Mech.* **67**, 85–111.

EAGLES, P. M. 1971 On stability of Taylor-vortices by fifth-order amplitude expansions. *J. Fluid Mech.* **49**, 529–550.

FRÊNE, J. & GODET, M. 1971 Transition from laminar to Taylor-vortex flow in journal bearings. *Tribology* **4**, 216–217.

FRÊNE, J. & GODET, M. 1974 Performance of plain journal bearings operating under vortex flow conditions. *Trans. A.S.M.E., J. Lub. Tech.* F **96**, 145–150.

JACKSON, P. A. & MOBBS, F. R. 1975 Visualisation of secondary flow phenomena between rotating cylinders. *3rd Symp. Flow Visualization, ISAS, Univ. Tokyo*, pp. 125–130.

JACKSON, P. A., ROBATI, B. & MOBBS, F. R. 1977 Secondary flows between eccentric rotating cylinders at sub-critical Taylor numbers. In *Super Laminar Flow in Bearings. 2nd Leeds–Lyon Symp. Tribology* (ed. D. Dowson, M. Godet & C. M. Taylor), pp. 9–14. London: Inst. Mech. Engrs.

KAMAL, M. M. 1966 Separation in the flow between eccentric rotating cylinders. *Trans. A.S.M.E., J. Basic Engng* D **88**, 717–724.

KENNETT, R. G. 1974 On the modulations and nonlinear interactions of waves and the nonlinear stability of a near-critical system. *Stud. Appl. Math.* **53**, 317–336.

KOSCHMIEDER, E. L. 1976 Taylor vortices between eccentric cylinders. *Phys. Fluids* **19**, 1–4.

MARKHO, P. H., JONES, C. D. & MOBBS, F. R. 1977 Wavy modes of instability in the flow between eccentric rotating cylinders. *J. Mech. Engng Sci.* **19**, 76–80.

REYNOLDS, O. 1886 On the theory of lubrication and its application to Mr Beauchamp Tower's Experiments, including an experimental determination of the viscosity of olive oil. *Phil. Trans.* **177**, 157–234. (See also *Papers on Mechanical and Physical Subjects*, vol. 2, pp. 228–310. Macmillan, 1901.)

STUART, J. T. 1958 On the non-linear mechanics of hydrodynamic stability. *J. Fluid Mech.* **4**, 1–21.

STUART, J. T. 1960 On the non-linear mechanics of wave disturbances in stable and unstable parallel flows. *J. Fluid Mech.* **9**, 353–370.

STUART, J. T. 1977 Bifurcation theory in non-linear hydrodynamic stability. In *Applications of Bifurcation Theory* (ed. P. H. Rabinowitz). *Proc. Adv. Seminar, Math. Res. Center, Univ. Wisconsin*, 1976, pp. 127–147. Academic Press.

VERSTEEGEN, P. L. & JANKOWSKI, D. F. 1969 Experiments on the stability of viscous flow between eccentric rotating cylinders. *Phys. Fluids* **12**, 1138–1143.

VOHR, J. A. 1967 Experimental study of super laminar flow between non-concentric rotating cylinders. *N.A.S.A. Contractor Rep.* no. 749.

VOHR, J. A. 1968 An experimental study of Taylor vortices and turbulence in flow between eccentric rotating cylinders. *Trans. A.S.M.E., J. Lub. Tech.* **F90**, 285–296.

WOOD, W. W. 1957 The asymptotic expansions at large Reynolds numbers for steady motion between non-coaxial rotating cylinders. *J. Fluid Mech.* **3**, 159–175.

ZARTI, A. S., JONES, C. D. & MOBBS, F. R. 1977 The influence of cylinder radius ratio on the variation of critical Taylor number with eccentricity ratio. In *Super Laminar Flow in Bearings. 2nd Leeds–Lyon Symp. Tribology* (ed. D. Dowson, M. Godet & C. M. Taylor), pp. 23–27. London: Inst. Mech. Engrs.